Toxicity and Bioaccumulation of Copper in *Phaeodactylum tricornutum* Under Different Macronutrient Conditions

Beibei Zhou[1], Yue Zou[2], Jie Ma[2], Yanping Li[2] and Ke Pan[2]*

[1] School of Life Sciences, Nantong University, Nantong, China, [2] Shenzhen Key Laboratory of Marine Microbiome Engineering, Institute for Advanced Study, Shenzhen University, Shenzhen, China

In this study, we investigated cell physiological and biochemical responses to copper (Cu) accumulation in the marine diatom *Phaeodactylum tricornutum* under different nitrogen (N) and phosphorus (P) conditions. Cells with sufficient N and P (+N+P) showed the highest total Cu concentrations and displayed a higher metal-tolerance ability. In the +N+P treatments, 36.5% of dissolved Cu was adsorbed on the frustules (cell walls), 54.9% was occluded in organelles, and 8.6% was in the soluble fraction. In comparison, cells with N and/or P shortages (+N−P, −N+P, and −N−P) adsorbed 10.8–13.1% of the total Cu onto their cell walls, 74.5–80% was occluded in organelles, and 9.2–12.4% was in the soluble fraction. The Cu^{2+} influx on the +N+P cell wall was faster due to sufficient metal ligands on the cell walls and up-regulated metal-related transporters. A significant increase in protein content occurred under N and/or P shortages, which was accompanied by the inhibition of the antioxidative enzymatic system and cell membrane damage. Our findings indicate that N and P play an important role in both Cu adsorption (cell surface) and uptake (intracellular), and they provide multifaceted evidence of the Cu acquisition mechanism in *P. tricornutum* under different macronutrient conditions.

Keywords: marine diatom, macronutrients, copper, metal accumulation, frustule

INTRODUCTION

Diatoms are unicellular photosynthetic eukaryotes that are responsible for 20% of global net primary productivity and up to 40% of all photosynthetic carbon fixation in the sea, and thus, they are crucial for the global carbon cycle (Nelson et al., 1995; Falkowski et al., 2005). Diatoms utilize nutrients such as nitrogen (N), phosphorus (P), silicon (Si), and iron (Fe) to maintain their cell cycle (Maldonado and Price, 1996; Litchman et al., 2006). Limitations to one of these elements can significantly influence nutrient uptake, cell growth, metabolism, and the composition of the cell constituents (Xin et al., 2010; Bromke et al., 2015).

It is well known that algae are resistant to heavy metals and can accumulate large, especially in the case of diatoms such as *Cylindrotheca fusiformis*, *Phaeodactylum tricornutum*, *Skeletonema costatum*, and *Thalassiosira pseudonana* (Bræk et al., 1980; Morelli and Pratesi, 1997; Pistocchi et al., 2000). This may be attributable to the peculiarity of their siliceous cell wall, known as the

frustule. The diatom frustule is a mixture of silica, proteins, and carbohydrates, and it is commonly used as a material to adsorb heavy metals (Zhao et al., 2019). In living cells, however, accumulation is a consequence of both passive adsorption onto the cell walls and active uptake into the cell (Ting et al., 1989). A complex network of metal transport, chelation, trafficking, and storage processes allows plants and algae to maintain micronutrient metal homeostasis and cope with the deleterious effects of excessive metals (Hanikenne et al., 2005).

Estuarine and coastal marine ecosystems can display phosphorus-limitation, nitrogen-limitation, and co-limitation, depending on inputs from agriculture, sewage, or rivers (Conley et al., 2009). Phosphorus is often the limiting nutrient in many regions of the ocean due to its fast recycling and effects on diatom growth and productivity (Alipanah et al., 2018), while N limitation can reduce the cellular pool sizes of glutathione (GSH) and phytochelatins (PCs), strongly inhibiting metal accumulation and enhancing metal toxicity (Miao and Wang, 2006; Rosenwasser et al., 2014). Nevertheless, the biochemical composition of algae varies under different nutrient conditions (Harrison et al., 1990). For instance, the major metal binding sites in the cell wall include carboxyl, ether, alcoholic, hydroxyl, and amino functional groups (Gélabert et al., 2006; Lim et al., 2008). Therefore, different nutrient-conditioned phytoplankton may have different metal sensitivities. A few studies have suggested that metal toxicity to phytoplankton may be dependent on the ambient nutrient concentrations, but consistent results have not been obtained. Wang and Dei (2001) demonstrated that N limitation can strongly suppress metal accumulation, while P had little effect. In contrast, Rijstenbil et al. (1998) found that the diatom *T. pseudonana* was more sensitive to Cu under P deficiency, as the Cu exclusion/elimination systems may be impaired. Therefore, metal toxicity to phytoplankton may be a metal-species-specific phenomenon. However, more microscale and subcellular analyses are needed to better elucidate metal toxicity to diatoms.

Phaeodactylum tricornutum is a model diatom for large-scale molecular analyses due to its published genome sequence and a well-developed molecular toolkit (Bowler et al., 2008; De Riso et al., 2009). In recent years, a number of membrane transport-protein families have been implicated in metal homeostasis in plants (Brembu et al., 2011; Takahashi et al., 2011; Milner et al., 2013). In this study, we investigated the expression of the metal-related genes responsible for Cu chelation, uptake, sequestration, and pumping with a combination of physiological and biochemical analyses to compare *P. tricornutum* under different macro-nutrient growth conditions.

MATERIALS AND METHODS

Culture Conditions
The *P. tricornutum* stock cultures were obtained from the Center for Collections of Marine Algae at Xiamen University (CCMA, Xiamen, China) and maintained under axenic conditions in f/2 medium at 23 ± 0.5°C with a light: dark cycle of 14: 10 h (light illumination of 100 µmol photons·m^{-2}·s^{-1}).

All seawater used in the metal toxicity experiments was passed through a Chelex ion exchanger (Bio-Rad) to remove trace metals, filtered through a 0.22-µm acetic fiber membrane (GP Express PLUS Membrane, Sericup, Millipore Corporation), and sterilized. The experiment was designed to investigate the effects of the phosphate and nitrate status (N- and P-enriched cells, N-starved cells, P-starved cells, and N- and P-starved cells) on copper accumulation. For the NP-enriched treatment, algae were acclimatized with the standard nitrate and phosphate concentrations in f/2 medium (Control; 883 and 36 µM, respectively). For N- and/or P-starvation, the nutrient concentrations maintained during the acclimation period were at f/20 levels of N (88.3 µM) and/or P (3.6 µM), respectively. Altered nutrient (N, P) ratios and limiting nutrient supplies can simulate the nitrogen limitation (-N+P), the phosphorus limitation (+N-P), and both the nitrogen and phosphorus limitation (-N-P) conditions in the natural water. Other major nutrients (e.g., Si, trace metals, and vitamins) were kept at the same f/2 levels used for the NP-enriched acclimation. All the flasks of microalgae were shaken twice a day by hand and acclimated for one month prior to the experiments.

Cell Growth and Toxicity Measurements
To investigate the effects of N and P on the cell growth conditions, the cell density was monitored daily for 7 days using a Bürker–Türk counting chamber (Karl Hecht KG, Sondheim, Germany). The cell-specific growth rate (µ) was calculated according to µ = ln $(C_{t2}/C_{t1})/(t_2 - t_1)$, where C_{t1} and C_{t2} are the cell densities at times *t1* and *t2*, respectively (Miao and Wang, 2006).

To determine the influences of the macronutrients N and P on metal adsorption, acclimated diatom cells were exposed to different Cu concentrations (0, 0.1, 1.0, 10.0, 20, 40, and 80 µM). The total dissolved-metal concentrations were determined using inductively coupled plasma-mass spectrometry (ICP-MS). Diatom cells in the mid-exponential growth phase were filtered (<50 mmHg vacuum) and then resuspended in nutrient-enriched or -starved resin-treated filtered seawater containing the different Cu concentrations. The initial cell densities were 1×10^6 cells·mL^{-1}, and all treatments were replicated three times.

After 96 h of exposure, the cell viabilities were examined with a plant cell viability assay kit (Sigma-Aldrich, USA) that simultaneously stains the cells with fluorescein diacetate (FDA) and propidium iodide (PI) dyes, which indicate viability and nonviability, respectively. The dyed diatom cells (per the manufacturer instructions) yield green (viable) and red (nonviable) fluorescence which can be detected under a fluorescent microscope (Axio Imager M2, ZEISS, Germany). The median lethal concentrations (LC50) were calculated using a linear interpolation method in an ICPIN software package (v2.0, U.S. Environmental Protection Agency, Duluth, MN).

Cellular Accumulation and the Partitioning of Dissolved Cu in *P. tricornutum*
At the end of the 96 h exposure to sub-lethal doses of total dissolved Cu (11.9 µM), an aliquot of 1 × 10^7 cells was removed

from each treatment, separated from the medium by centrifugation ($2630 \times g$ at 4°C), and washed 3 times with 0.22 µm-filtered seawater. A part of the algae was used to analyze the total accumulation of heavy metals, and the other part was used to analyze the subcellular distribution of the Cu. For the subcellular analysis, the cells were then washed 3 times with 100 mL of 1 mmol·L^{-1} EDTA (pH = 7.0) to remove any Cu^{2+} loosely bound to the cells' exteriors (Campbell and Smith, 1986). To further separate the Cu into the different subcellular partitions, the pellets were transferred to 1.5 mL tubes and homogenized in Tris–HCl buffer (10 mmol·L^{-1}, pH = 7.4) with an ultrasonic homogenizer (Wiggen Hauser, GM3100, Berlin, Germany) for 5 min (3 s pause after each 3 s pulse) in an ice bath. The homogenate was centrifuged at $1000 \times g$ for 30 min to obtain pellets containing the cell-adsorbed fraction. The supernatant was then centrifuged at $65,000 \times g$ for 30 min to separate the insoluble organelles (pellet) from the soluble substances (supernatant) (Weigel and Jger, 1980; He et al., 2008; Wang and Wang, 2008). The pellets were then freeze-dried and digested with 0.5 mL concentrated nitric acid (70%; Sigma-Aldrich) at 100°C for 24 h. Metal contents in the insoluble organelles and soluble fractions were measured using inductively coupled plasma mass spectrometry (ICP-MS; Agilent 7900).

Measuring Net Cu^{2+} Flux With Non-Invasive Micro-Test Technology

The net fluxes of Cu^{2+} around the diatom cells were measured using non-invasive micro-test technology (NMT; BIO-IM, YoungerUSA, LLC, Amherst, MA 01002, USA) as described in our previous study (Zhou et al., 2020). Briefly, when Cu^{2+} is adsorbed by cells, the Cu^{2+} concentration increases gradually from near the cell membrane to the periphery, with the direction of Cu^{2+} inflow defined as negative. Conversely, when Cu^{2+} is released from cells, the direction of Cu^{2+} efflux is defined as positive. Before testing, ion selective microelectrodes were calibrated using 10 µM Cu^{2+} ion solutions to ensure the electrode test values were within the normal range, and only electrodes with Nernstian slopes >25 mV/decade were used (Li et al., 2017). The electrode was mounted on a 3-dimensional micro-manipulation device on a microscope, with the diatom (mid-exponential growth phase) placed at the center of the stage. The electrode tip was connected to the bath solution and positioned 2–3 µm above the diatom surface before measuring the electrochemical gradients at two points near and away from the cell (excursion distance 10 µm; frequency 0.2–0.3 Hz). The raw data were processed to obtain the ion mobility rates and units (pmol·cm^{-2}·s^{-1}) using Fick's first law of diffusion equation: $J = -D_0(dc/dx)$, where J is the ion flux (pmol·cm^{-2}·s^{-1}), D_0 is the ionic diffusion constant (7.14×10^{-5} cm^2·s^{-1} for Cu), dc is the ion concentration gradient, and dx is the excursion distance (i.e., the microelectrode movement). Testing was conducted at 20–23°C, and six replicate measurements were obtained for each treatment.

X-Ray Photoelectron Spectroscopy (XPS) Analysis of the Cell Wall

For the XPS analysis, samples cultured with and without Cu under different N and P conditions were frozen at −20°C and freeze-dried; XPS was then used to characterize the binding states of carbon (C 1s), oxygen (O 1s), silicon (Si 2p), nitrogen (N 1s), phosphorus (P 2p), sulfur (S 2p), and calcium (Ca 2p) on the cell surfaces. The lyophilized diatoms were placed on an aluminum platform for the XPS (VG MultiLab, 2000, Thermo VG Scientific; East Grinstead, West Sussex, UK) measurements using an Al Ka X-ray source (1486.6 eV) at 300 W. Photoelectrons were collected at a take-off angle of 53° for a sampling depth of ~10 nm. All experiments were conducted in triplicate. The binding energy of the spectra was standardized with the neutral C (1s) peak at 284.7 eV, and the background was linearly subtracted (Cicco et al., 2016). Thermal Advantage software was used to fit the XPS spectra peaks, which were fitted with a number of known components with similar full width at half maximum measurements. Peak positions within 0.5 eV were identified as the same.

RNA Isolation and Real-Time PCR

To identify the different rates of Cu internalization in *P. tricornutum* under nutrient-enriched and nutrient-starved conditions, we examined the expression of several cell membrane transporters related to Cu uptake, efflux, and storage and one metal-chelation protein on the cell wall. The ZIP-T1 (Zrt-, Irt-like Protein) transporter is responsible for moving multiple divalent metal cations such as Fe, Zn, Mn, Co, Cu, or Cd into the cytoplasm (Blaby-Haas and Merchant, 2012). Frustulin (Fru5-1) is a protein on the outermost cell wall of diatoms that has an affinity for Cd and other metal bindings, thereby decreasing metal bioavailability and uptake (Kröger et al., 1994; Kröger et al., 1996; Kröger et al., 1997; Santos et al., 2013). The P$_{1B}$-type ATPase (ATPase5-1B) was recognized as a copper transporter and is responsible for providing Cu to organelles and mediating copper excess when present (La Fontaine and Mercer, 2007). Another transporter, VIT1 (Vacuolar Iron Transporter 1), mediates vacuolar metal storage (Kim et al., 2006).

After exposure to the same metal concentrations used in the subcellular Cu-accumulation experiments, *P. tricornutum* cells were harvested by centrifugation at $2630 \times g$ for 10 min at 15°C. The cell pellets were resuspended in 1 mL filtered seawater, transferred to 2 mL tubes, and centrifuged again at $18,000 \times g$ for 1 min at 4°C. The resulting supernatants were discarded, and the cell pellets were flash frozen in liquid nitrogen and stored at −80°C until use.

Total RNA was extracted using the RNeasy Plant Mini Kit (Qiagen, Valencia, CA, USA) according to the manufacturer instructions. Reverse transcription reactions were performed with 0.5 µg RNA using PrimeScript^{TM} RT Master Mix (Takara, Kyoto, Japan). A quantitative real-time PCR (qRT-PCR) analysis was performed using SYBR Premix Ex Taq^{TM} II (Takara, Kyoto, Japan) on a LightCycler$^{®}$ 96 instrument (Roche Diagnostics, Mannheim, Germany). The qRT-PCR primers used for the genes ZIP-T1, Fru5-1, ATPase5-1B, VIT1, and β-actin (internal control) are shown in **Table S1**. The relative mRNA expression was determined using the $2^{-\Delta\Delta CT}$ method (Livak and Schmittgen, 2001). Three independent biological replicates were used in all experiments.

Intracellular Proteins and Antioxidant Responses

After the 96 h incubations, the total protein contents and the antioxidant enzyme activities were determined. A total of 4×10^7 P. tricornutum cells were collected and disrupted for 6 min in an ice-cold buffer solution (50 mM K_2HPO_4, 0.1 mM EDTA; pH 7.8) using an ultrasonic homogenizer (Wiggen Hauser, GM3100, Berlin, Germany). Each 3 s homogenization was followed by a 3 s pause to prevent the possible inactivation of proteins due to a temperature increase during the extraction. After centrifuging the homogenate (2013 × g at 4°C for 10 min), the supernatant was used to determine the protein concentrations and antioxidant enzyme activities. The protein concentrations were quantified at 595 nm using bovine serum albumin (BSA) as the standard (Bradford, 1976), and the results are expressed in milligrams protein per million cells (mg protein/ M cells).

Superoxide dismutase (SOD) activity was measured based on the inhibition of nitro blue tetrazolium reduction by superoxide radicals generated with xanthine/xanthine oxidase (Giannopolitis and Ries, 1977; Misra and Gupta, 2006). The SOD activity values are expressed as $U \cdot mg^{-1}$ protein. To assess membrane damage in the diatom cells, the lipid peroxidation/ malondialdehyde (MDA) concentration was measured using an absorption coefficient of 155 $mM^{-1} \cdot cm^{-1}$ and is expressed as $nmol \cdot mg^{-1}$ protein. Glutathione (GSH) is a substrate for PC synthesis and is crucial for the detoxification of heavy metals (Hasanuzzaman et al., 2017). The cellular SOD activity and MDA and GSH content in each sample were determined using corresponding kits purchased from Jiancheng Biotech (Nanjing, China) following the manufacturer instructions.

Statistical Analysis

Data were analyzed using a one-way analysis of variance (ANOVA) followed by Duncan *post hoc* multiple-comparison tests (SPSS 16.0 software). Significant differences were accepted for $p < 0.05$.

RESULTS

Cell Growth and Cu Toxicity Analysis

The growth curves for P. tricornutum under different N/P concentrations are shown in **Figure 1**. Clear significant growth inhibition was observed for the +N−P, −N+P, and −N−P treatments relative to the control (+N+P). The growth rates did not significantly differ between the +N−P and −N+P treatments, which had cell-specific growth rates of 1.5 and 1.4, respectively. For the cells grown under the −N−P conditions, growth was severely inhibited, by 91% relative to the +N+P cells (**Figure 1A**).

The cell viability of the P. tricornutum cells exposed to different levels of Cu is shown in **Figure 1B**. As the metal concentration increased, the inhibitory effects of Cu on P. tricornutum's growth increased. The concentration which gives a 50% effect (EC50) in the +N+P, +N−P, −N+P, and −N−P cells after 96 hours were 16.73, 15.70, 13.02, and 10.33 μM, respectively.
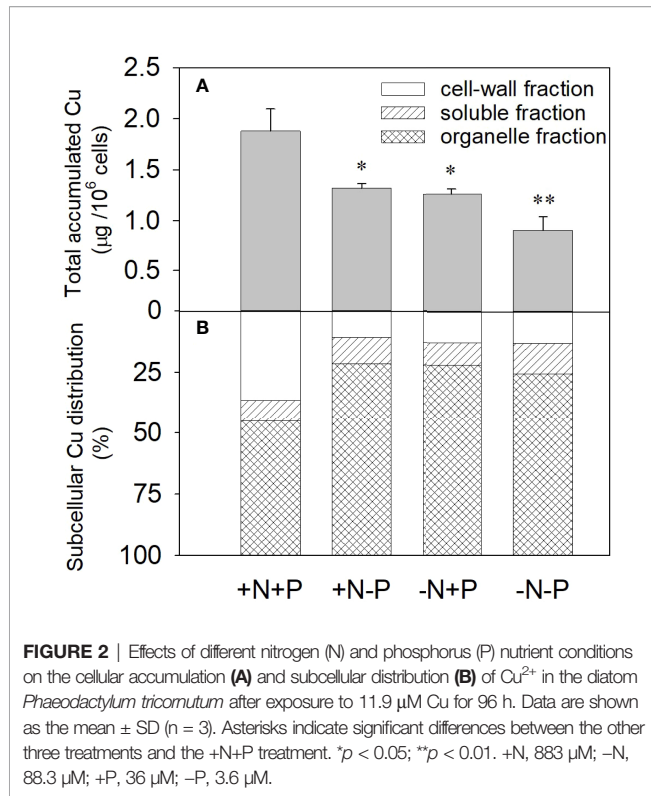
N/P-Dependent Accumulation and Subcellular Distribution of Cu in *P. tricornutum*

After being treated with 11.9 μM Cu for 96 h, the accumulated Cu in the +N+P cells was 1.88 μg/10^6 cells, which was significantly higher than that in the cells grown with an N and/or P deficiency. The amounts of accumulated Cu in the +N−P and −N+P cells were 1.32 and 1.26 μg/10^6 cells, respectively, while the amount in the −N −P cells was only about half (0.90 μg/10^6 cells) that in the +N+P treated cells (**Figure 2A**).

The results of the copper subcellular fractionation for the four treatments after the 96 h toxicity test are shown in **Figure 2B**. For cells under N- or P-depleted conditions, most of the accumulated Cu was distributed in the insoluble organelle fraction, while in the +N+P cells, the subcellular distribution changed, with increased Cu in the cell-wall fraction. Compared with the N- or P-limited cells, the −N−P cells exhibited a higher concentration of accumulated Cu in the soluble fraction. For the −N/−P treatments, 74.5–78.5% of the accumulated Cu was localized in the cell organelles, 9.2–12.4% was in the soluble fraction, and <13.1% was associated with the cell
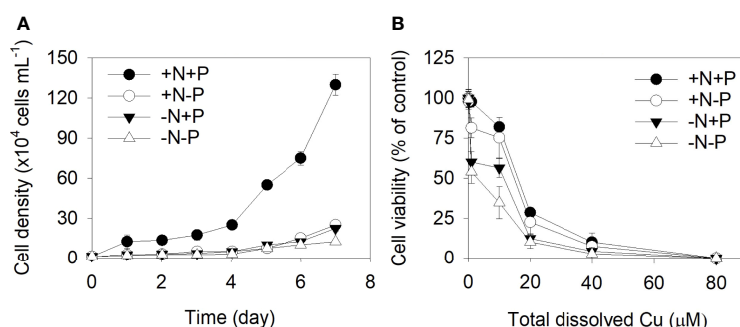
FIGURE 1 | **(A)** Effects of different nitrogen (N) and phosphorus (P) supplies on the cell density of *Phaeodactylum tricornutum*. **(B)** N- and/or P-dependent cell viability after a 96 h exposure to varying concentrations of Cu (0, 0.1, 1.0, 10.0, 20.0, 40.0, and 80.0 μM). +N, 883 μM; −N, 88.3 μM; +P, 36 μM; −P, 3.6 μM. Data are shown as the mean ± SD (n = 3).

FIGURE 2 | Effects of different nitrogen (N) and phosphorus (P) nutrient conditions on the cellular accumulation **(A)** and subcellular distribution **(B)** of Cu^{2+} in the diatom *Phaeodactylum tricornutum* after exposure to 11.9 µM Cu for 96 h. Data are shown as the mean ± SD (n = 3). Asterisks indicate significant differences between the other three treatments and the +N+P treatment. *$p < 0.05$; **$p < 0.01$. +N, 883 µM; −N, 88.3 µM; +P, 36 µM; −P, 3.6 µM.

membrane and/or cell wall. In comparison, in the +N+P cells, 37% of the accumulated Cu was distributed to the cell membrane and/or cell wall, 45% was located in the organelle fraction, and 18% was in the soluble fraction. The XPS results showed that a considerable fraction of Cu was adsorbed on the cell surface under sufficient N and P conditions relative to when N and/or P were deficient.
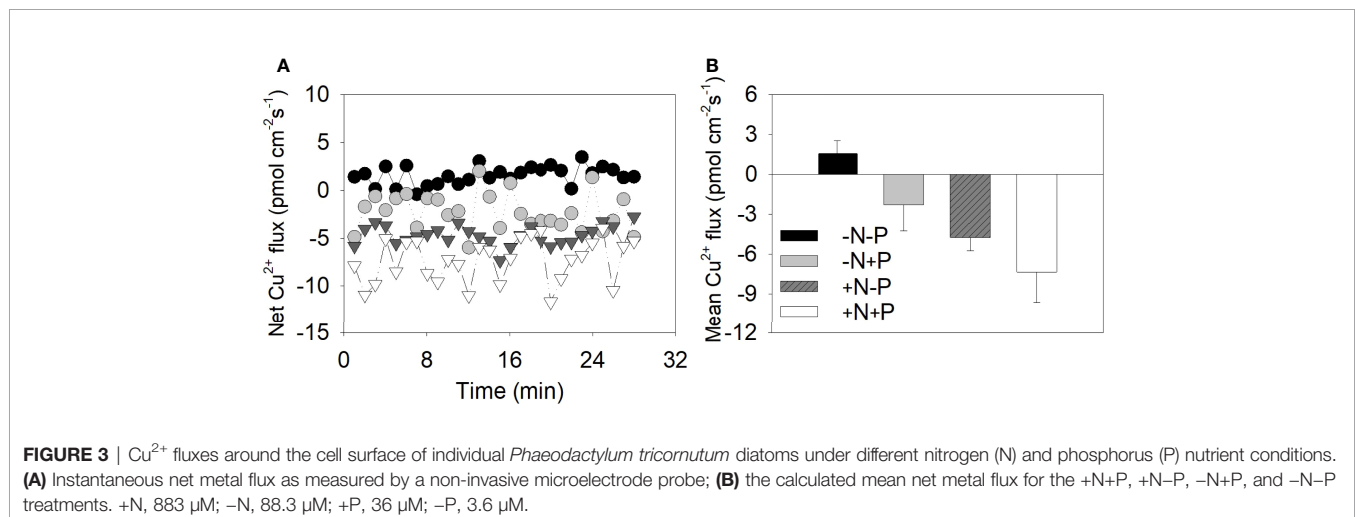
Net Cu^{2+} Flux in *P. tricornutum*

To further explore the differences in the uptake abilities of the cell walls under different N conditions, we used NMT to investigate the Cu^{2+} flux around individual diatom cell

surfaces. Negative and positive flux values suggest ion influx onto cell surfaces and efflux from the cell, respectively. The metal flux values varied between −0.42 and 3.46 (average 1.56 ± 0.95) $pmol \cdot cm^{-2} \cdot s^{-1}$ for the −N−P cells, between −11.65 and −3.96 (average −7.33 ± 2.24) for the +N+P cells, between −5.98 and 2.02 (average −2.27 ± 1.94) $pmol \cdot cm^{-2} \cdot s^{-1}$ for the −N+P cells, and between −7.33 and −2.76 (average −4.73 ± 1.00) $pmol \cdot cm^{-2} \cdot s^{-1}$ for +N−P cells (**Figures 3A, B**).

Cell Surface Chemical Composition

X-ray photoelectron spectroscopy was performed to further analyze the chemical composition changes on the cell surface before and after Cu adsorption and interactions between the functional groups and heavy metal ions. The wide scan XPS spectra of the cell surface showed that the atomic percentages for O, C, Mg, Si, and N contributed more than 98% of the detected elements (**Table 1**). Before the Cu addition, the C/O ratios in the +N+P and +N−P cells were 2.03 and 2.14, respectively, lower than those in the −N+P (3.95) and −N−P (3.73) cells.

After Cu exposure, magnesium decreased in the P-limited cells, calcium decreased in the N-limited cells, and both magnesium and calcium decreased in the −N−P cells, whereas in the +N+P cells, there was no change in calcium and an increase in magnesium (**Table 1**). The decrease in magnesium and/or calcium was due to the competition of Cu for ion exchange sites under N and/or P shortage. High resolution spectra of the O1s and C1s regions are shown in **Figure 4**. The peaks with a binding energy of 531.3/531.4 eV can be assigned to oxygen atoms in the form O=C (carboxyl and/or quinone groups), while those at 532.6/532.7 eV can be assigned to oxygen atoms in the form O–C (ether and/or alcohol hydroxyl). These two assignments reflect the functional groups in the cell wall. **Figures 4E–H, M–P**) shows that the binding energies of the peaks on the cell walls have a certain degree of shift before and after Cu adsorption. After Cu exposure, the quantity of C=O groups increased from 58.0% to 73.2% in the +N+P cells, from 38.1% to 50.9% in the −N+P cells, and from 27.6% to 29.5% in the −N−P cells, which were obviously accompanied by decreases in the C-O groups (**Figures 4M, O, P**).

FIGURE 3 | Cu^{2+} fluxes around the cell surface of individual *Phaeodactylum tricornutum* diatoms under different nitrogen (N) and phosphorus (P) nutrient conditions. **(A)** Instantaneous net metal flux as measured by a non-invasive microelectrode probe; **(B)** the calculated mean net metal flux for the +N+P, +N−P, −N+P, and −N−P treatments. +N, 883 µM; −N, 88.3 µM; +P, 36 µM; −P, 3.6 µM.

TABLE 1 | X-ray photoelectron spectroscopy (XPS) spectral parameters of the cell surfaces of diatoms (*Phaeodactylum tricornutum*) cultured under four different nitrogen (N) and phosphorus (P) nutrient conditions: +N+P, −N+P, +N−P, and −N−P.

Valence state	Metal treatment	Assignment[a]	+N+P[b]			+N−P			−N+P			−N−P		
			AP (%)	BE (eV)	CD (%)	AP (%)	BE (eV)	CD (%)	AP (%)	BE (eV)	CD (%)	AP (%)	BE (eV)	CD (%)
C1s	−Cu	C–(C, H)[1,2]	57.87	284.7	62.7	59.46	284.7	62.2	75.77	284.7	64.4	74.09	284.8	69.1
		C–(O, N)[3,4]		286.1	22.9		286.1	25.3		286.0	30.4		286.1	20.6
		O–C–O, C=O[2,4]		288.0	14.4		288.0	12.4		287.9	3.0		288.0	10.3
										288.9	3.1			
	+Cu	C–(C, H)[1,2]	53.46	284.7	67.8	71.02	284.7	65.0	67.09	284.7	62.1	71.96	284.7	59.4
		C–(O, N)[3,4]		286.1	20.0		286.2	24.2		286.1	24.3		286.1	28.5
		O–C–O, C=O[2,4]		288.0	12.1		288.0	10.8		288.0	13.6		288.0	12.1
O1s	−Cu	O=C,[6]	28.49	531.3	58.0	27.83	531.3	55.0	19.19	531.4	38.1	19.84	531.4	27.6
		O–C[4,7,8]		532.6	42.0		532.6	45.0		532.6	61.9		532.6	72.4
	+Cu	O=C[6]	31.06	531.3	73.2	21.86	531.3	41.5	24.91	531.3	50.9	21.67	531.4	29.5
		O–C[4,7,8]		532.7	26.8		532.6	58.5		532.6	49.1		532.6	70.5
Si2p	−Cu	Si–OH[2,4]	1.24	102.2	88.5	2.55	102.2	75.5	1.03	102.2	83.9	1.14	102.2	80.1
		SiO_2[2,4]		103.2	11.5		103.1	24.5		103.1	16.1		103.1	19.9
	+Cu	Si–OH[2,4]	1.71	102	98.4	1.23	102.1	90.1	1.56	102.2	88.8	0.81	102.1	72.1
		SiO_2[2,4]		103.3	1.6		103.2	9.9		103.1	11.2		103.1	27.9
N1s	−Cu	N_{nonpr}[9]	4.89	399.8	100	4.27	399.9	100	1.21	399.9	93.3	2.44	399.9	100
		N_{pr}[2]								402.1	6.7			
	+Cu	N_{nonpr}[9]	3.79	399.9	97.2	3.84	399.9	98.8	3.2	399.9	99	3.67	399.9	94.2
		N_{pr}[2]		402.1.	2.8		402.1	1.2		402.1	1		402.1	5.8
P2p	−Cu		0.48			0.12			0.4			0.26		
	+Cu		0.59			0.26			0.65			0.31		
S2p	−Cu	SO_4^{2-}[2]	0.44			0.45			0.36			0.5		
	+Cu	SO_4^{2-}[2]	0.52			0.59			0.48			0.54		
Mg2p	−Cu		6.6			5.32			1.5			1.49		
	+Cu		8.87			1.05			1.98			0.9		
Ca2s	−Cu		–			–			0.53			0.24		
	+Cu		–			0.15			0.12			0.14		

[a]The references for the assignment of binding energies are shown in the supporting information.

[b]+N, 883 µM; −N, 88.3 µM; +P, 36 µM; −P, 3.6 µM; +Cu, 11.9 µM; −Cu, no Cu addition.

[1.]Raveendran et al., 2015; [2]Cicco et al., 2016; [3]Dufrene et al., 1997; [4]Tesson et al., 2009; [5]Nohira et al., 2002; [6]He et al., 2013; [7]Jedlicka et al., 2007; [8]Condorelli et al., 2004; [9]Boukherroub et al., 2000.

AP, atomic percentage; BE, binding energy; CD, component distribution, that is, the proportion of each component peak.

However, there was an opposite trend in the +N−P treated cells, with the quantity of C=O groups decreasing and C-O groups increasing (**Figures 4G, O**).

The C1s spectra produced three peaks with three binding energies (**Figures 4A–D, I–L**). These peaks can be assigned to C atoms in the forms of C-(C, H), C-(O, N), and O-C-O (ether or C=O) groups. Overall, the peaks of the single-bonded carbon C-(O, N) after Cu sorption were less than that before sorption in treatments +N+P (22.9 vs 20.0%), +N-P (25.3 vs 24.2%), and -N+P (30.4 vs 24.3%), and these were consistent with the findings from the O1s spectra. The −N −P-treated cells showed the lowest concentration of C-(O, N) groups before Cu addition (**Figure 4D**), and both the C-(O, N) and O-C-O (ether or C=O) forms increased after Cu exposure (**Figure 4L**).

The Si2p spectra produced two peaks, which can be assigned to amorphous silicate (Si-OH) and silica (SiO₂) groups. Initially, the cells grown with limited N and/or P had a lower proportion of Si-OH groups and higher proportion of SiO₂ (**Table 1**). After Cu adsorption, the Si-OH/SiO₂ ratios sharply increased from 7.7 to 61.5 in the +N+P cells, from 3.8 to 9.1 in the +N−P cells, and from 5.2 to 7.9 in the −N+P cells, whereas in the −N−P-treated cells, the ratio fell from 4.02 to 2.58.

Expression of Cu-Related Transporters and Genes

Metal-related transporter analyses can help us to understand the molecular events associated with the uptake, transport, and sequestration of metal ions. Therefore the relative gene expression levels of ZIP-T1, Fru5-1, ATPase5-1B, and VIT1 were examined in cells after chronic Cu exposure under different N/P ratios (**Figure 5**). Overall, N and/or P shortages had a strong negative effect on the detected gene expressions, with the genes consistently expressed at a higher level in the +N+P cells. The expression levels were the lowest when both N and P were limited. Comparing the N-limited cells with the P-limited cells showed that N-limited cells had higher ZIP-T1 expression (1.28-fold) and lower ATPase5-1B (0.91-fold) and Fru5-1 expression (0.77-fold) than P-limited cells.

Changes to Total Proteins and Intracellular Enzyme Activity

The total protein and antioxidant enzyme responses to further investigate how the cells detoxified intracellular Cu when under nutrient depletion were examined. In the +N+P cells, there were no significant changes in the total proteins under chronic Cu exposure. However, total proteins were significantly elevated in the
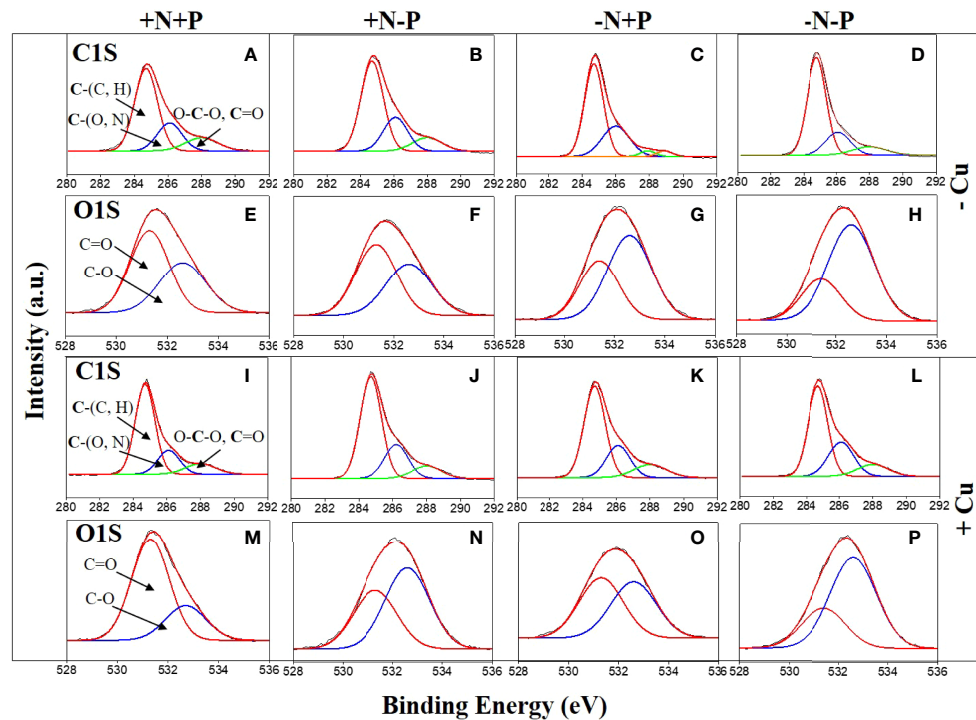
FIGURE 4 | High-resolution C,1s and O,1s X-ray photoelectron spectroscopy spectra of the diatom (*Phaeodactylum tricornutum*) cell wall of cells incubated for 96 h under different nitrogen (N) and phosphorus (P) nutrient conditions with (+Cu) and without (−Cu). C1s **(A–D)** and O1s **(E–H)** of the +N+P, +N–P, –N+P, and –N–P treatments without Cu exposure. C1s **(I–L)** and O1s **(M–P)** of the four treatments after Cu exposure. +N, 883 µM; –N, 88.3 µM; +P, 36 µM; –P, 3.6 µM.

cells with N and/or P shortages, with 2.6-, 3.8-, and 5.6-fold increases in the +N–P, –N+P, and –N–P cells, respectively (**Figure 6A**).

Under Cu treatment, the SOD activity slightly increased in the NP-enriched cells, but was significantly reduced in the cells with N and/or P shortages, with reductions of 47.4%, 67.4%, and 73.6% in the +N–P, –N+P, and –N–P cells, respectively (**Figure 6B**). In contrast, the MDA content increased in response to Cu stress in the +N–P, –N+P, and –N–P cells (1.3-, 1.6-, and 1.3-fold, respectively; **Figure 6C**). Upon exposure to Cu, the GSH content was reduced to between 16.2% and 36.9% of the total levels in the four treatments (**Figure 6D**).

DISCUSSION

N and/or P Shortages Reduced Cell Growth and Increased Metal Sensitivity in *P. tricornutum*

Our results showed that there was a strong relationship between the cell growth and N/P status, with both N and P limitations significantly reducing the cell growth and metal tolerance of *P. tricornutum*. Similar decreases in cell growth and cell density in response to N and/or P deficiency have been observed in the diatoms *Thalassiosira weissflogii* and *P. tricornutum* (Liu et al., 2011; Alipanah et al., 2018). Rijstenbil et al. (1998) reported that the diatom *T. pseudonana* was more Cu sensitive under nutrient

deficiency. In agreement with the previous authors, other studies have identified several specific metal toxicity to algae in more serious conditions namely induced by N and/or P shortages (Wang and Dei, 2006; Serra et al., 2010).
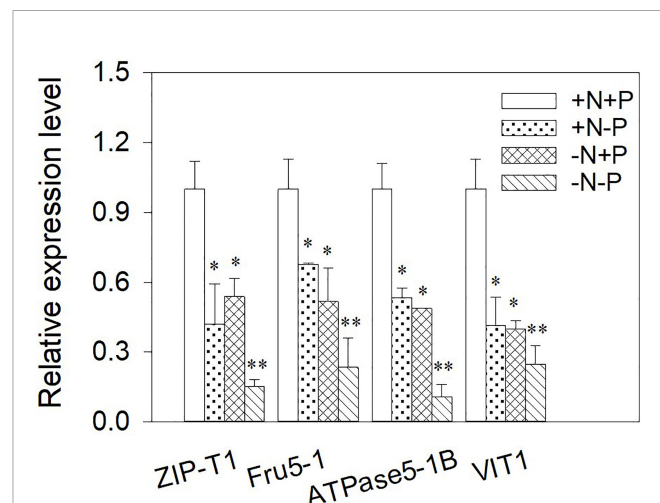

FIGURE 5 | Relative expression of genes in *Phaeodactylum tricornutum* cultured under different nitrogen (N) and/or phosphorus (P) nutrient conditions after a 96 h Cu exposure. The relative gene expression levels were calculated against β-actin. Asterisks indicate significant differences versus the control (+N+P) cells. *$p < 0.05$; **$p < 0.01$. +N, 883 µM; –N, 88.3 µM; +P, 36 µM; –P, 3.6 µM.

Explanations for these observations have been provided by both physiological and biochemical studies. One possible explanation is that because N is involved in protein synthesis, it can determine the concentration of protein ligands such as GSH and PCs, which are involved in intracellular metal binding and toxicity (Rosenwasser et al., 2014; Wu et al., 2019), whereas P participates in the secretion of extracellular polymeric substances from diatom cells that may be responsible for extracellular metal binding to reduce metal toxicity (Brembu et al., 2017). It has been shown that the uptake and metabolism of both N and P are suppressed during P deprivation (Alipanah et al., 2018). In addition, N and P availabilities change the properties and chemical components of the diatom frustule, which provides different metal-binding sites (Gélabert et al., 2007; Yap et al., 2016). In summary, N and P affect the metal toxicity to cells through extracellular, cell wall, and intracellular changes, but there is a lack of evidence to better understanding the interaction of these changes. In this paper, we tried to explain the observation of decreased cell growth and metal tolerance in diatoms under N and/ or P shortage by revealing that sufficient N and P guaranteed the number and diversity of metal-binding sites, support the normal expression of genes to transport and chelation metal on the cell walls, and thus the cell walls could bind more metal. Then the relatively high proportion of the total metal on the cell walls alleviated the stress of intracellular heavy metals on cells, which results in an improved effect of intracellular antioxidant enzyme systems on metal detoxification. Our study provided the first evidence in a chain reaction of how N and P regulate the adsorption, accumulation, and distribution of metals to affect the tolerance of cells to metals.

N/P Availability Increased Cu Accumulation by Distributing More Cu on the Cell Wall to Decrease Metal Toxicity

Nutrients such as N and P can significantly affect metal accumulation. Rijstenbil et al. (1998) found that the diatom *T. pseudonana* can accumulate more Cu in N-enriched media than in N-limited media. Similarly, Sivakumar et al. (2010) found that Cu accumulations were decreased with lower N concentrations. Miao and Wang (2006) found that Cd accumulation was inhibited under N-limited conditions. Furthermore, a study by Wang and Dei (2001) found that N addition significantly increased the accumulation of Cd due to higher rates of Cd uptake in the cells. Our results are consistent with these observations, with the accumulated Cu concentration in the diatom *P. tricornutum* being 2.1 times higher under NP-enriched conditions than under N and/or P shortages.

Further, the metal subcellular distribution assay showed that +N+P cells tend to distribute a larger proportion of Cu on the cell wall than the N- and/or P-deficient cells. A heavy metal subcellular distribution analysis helped to understand the mechanisms of metal accumulation, transport, and detoxification in plants (Lu et al., 2017). Our metal distribution analysis provided clues to explain why the +N+P cells accumulated more Cu content while having a lower Cu sensitivity. The intracellular distribution of Cu in the diatom *P. tricornutum* has an important effect on the metal sensitivity of the cells. Previous studies have found that the subcellular metal distribution (e.g., Cd and Cu distributions in the cell-surface-adsorbed, soluble, and insoluble fractions) is time-metal-species specific (Miao and Wang, 2006; Miao and Wang, 2007), but little
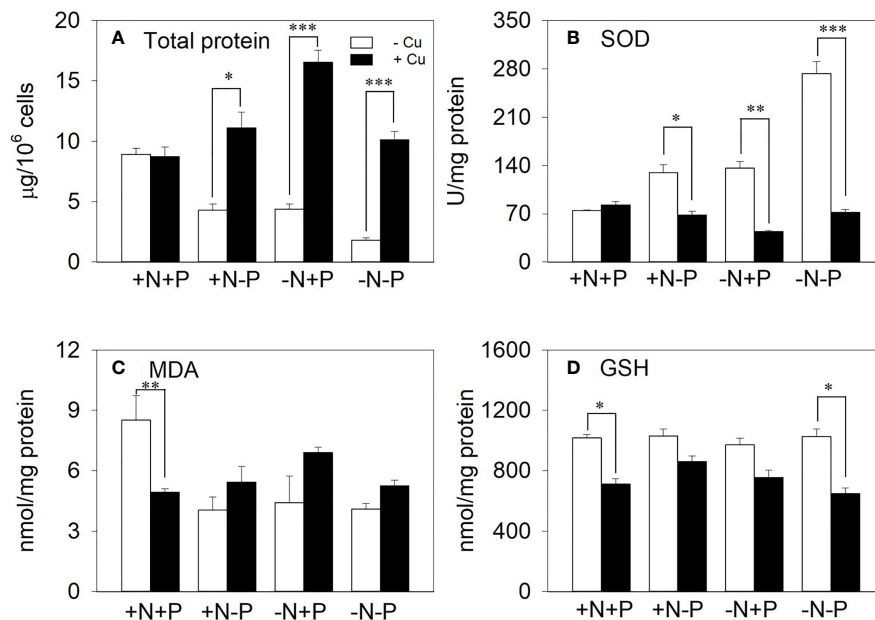
FIGURE 6 | The effect of different nitrogen (N) and phosphorus (P) supplies on **(A)** total protein, **(B)** superoxide dismutase (SOD), **(C)** malondialdehyde (MDA), and **(D)** glutathione (GSH) in the diatom *Phaeodactylum tricornutum* after a 96 h exposure to 11.9 μM Cu (mean ± SE). Asterisks indicate significant differences. *$p < 0.05$, **$p < 0.01$, ***$p < 0.001$. +N, 883 μM; –N, 88.3 μM; +P, 36 μM; –P, 3.6 μM.

attention has been paid to the role of the relative amount of heavy metals adsorbed to the cell wall in the diatom's defense against heavy metal toxicity. Our results suggest that the siliceous cell wall is a good defender against heavy metal toxicity and that the increased Cu distribution in the cell wall may alleviate Cu stress.

Influence of N/P-Dependent Cell Wall Chemical and Molecular Characteristics on Cu Adsorption

The different proportions of metals in the subcellular fractions caused a discrepancy in the cells' sensitivities to metals and led us to analyze the cell wall and intracellular changes under different N/P conditions. We examined the cell wall biochemical composition and characteristics through NMT, XPS, and molecular analyses. The NMT results indicated that the NP-available cells had a greater Cu uptake capacity than the N- and/or P-starved cells. The positive average values for the $-N-P$ cells suggest that the elimination of Cu^{2+} outcompeted its uptake under N and P restriction. Although the values for the +N+P, +N−P and −N+P cells were all negative, the +N+P cells exhibited 3.23 and 1.55-fold higher Cu^{2+} influx than the −N+P and +N−P cells, respectively, suggesting faster Cu^{2+} uptake than elimination during initial contact with the metal when both N and P are sufficient. A weaker influx rate of Cu into the cell wall of nutrient-deprived diatoms should be due to the lower C–O content in the carboxyl group and to Si–OH attached to Cu^{2+} on the cell wall, which was accompanied by the downregulation of a metal-binding protein and the suppression of metal transporters in the cell wall. The silanol (Si–OH) groups on the diatom cell walls control the surface charge properties and metal binding affinities (Gélabert et al., 2004). The smaller ratios for the cells under N- and/or P-deprivation indicated they had fewer Si–OH groups. The changes in the contents of C-O and C=O indicated that they were involved in the adsorption of Cu onto the cell surface (Lim et al., 2008). Metal toxicity to aquatic organisms depends on the speciation of the metal and its binding to biotic ligands (Levy et al., 2007; Adams et al., 2016). Research has examined the metal-binding ability of different ligands in the diatom cell wall and shown that multiple hydroxyl (–OH), carboxyl (–COOH), amino (–NH₂), and silanol (Si–OH) functional groups can enhance adsorption capabilities (Badruddoza et al., 2011; Marella et al., 2020). Before adding Cu, the cells had lower C and higher O concentrations on the +N cell walls than on +P cell walls. Avery and Tobin (1993) have shown that greater relative effects on the adsorption of the cations Cu^{2+} and Cd^{2+} are correlated with complexation by anions from oxygen-containing ligands. The low C/O ratio indicated that more oxygen-containing functional groups were present on the +N cells' surface for metal binding (Compton et al., 2011). Combined with the higher metal and O concentrations in the +N cells, it is clear that N plays a role in providing oxygen-linked binding sites for metal ions on the cell wall. The shift in the binding energies of C and O after Cu^{2+} adsorption is likely caused by the binding of copper ions onto their corresponding functional groups (mainly C-O), thus reducing the electron density. Similar observations that the relative C-O content is reduced and that C=O is increased after copper adsorption has been reported by Lim et al. (2008) and Zheng et al. (2009). Interestingly, we found that the increased C=O and decreased single bonded C-O only occurred in one of the C and O elements in cells under N and/or P limitation. This indicates that the cell wall

adsorption mechanism for Cu is more complicated under N- and/or P-deficient conditions than when N and P are sufficient. Judging from the decrease in calcium and magnesium on the diatom cell wall under N and/or P deficiency, we inferred that except for the chelate complexes, ion exchange might be another binding mechanism in those cells. For the +N+P treatment, the main Cu^{2+} binding mechanism by the diatom cell wall was forming chelate complexes with adequate carboxyl and Si-OH groups, and thus there was no need to perform ion exchange, which is in good agreement with our NMT results. In addition, Ma et al. (2018) found that after the Cu^{2+} adsorption, a lower density of silanol (Si-OH) groups was found in the cells with N and/or P shortages, demonstrating a weaker metal adsorption ability on the cell surfaces. A new binding energy at 402.1 was also observed by Badruddoza et al. (2011), which was assigned to protonated N and assumed to balance the electrical charges of the adsorbed copper ions.

The sequenced diatom *P. tricornutum* is a valuable model for marine phytoplankton studies (Armbrust et al., 2004), allowing us to better analyze the expression of annotated putative genes related to Cu transport and assimilation. In this study, the N and P availability affected the *P. tricornutum* involved in Cu assimilation and intracellular distribution gene expressions, with all the genes down-regulated in the N- and/or P-deficient cells relative to the +N+P cells. Besides, in P-limited cells, more Cu was sequestered in the frustule by Fru5-1 and less Cu was transported intracellularly in comparison with the N-limited cells. Frustulins, a major group of glycoproteins contain multiple acidic cysteine-rich domains (ACR domains), constitute and are located in the outer coat of the cell wall (Kröger et al., 1996). Santos et al. (2013) reported that diatom *Nitzschia palea* increased 6 times frustulins production due to the presence of Cd, and 85.4% of Cd was bound to the frustulin fraction. Moreover, C-O is the function group of ACR domains (Benesch and Benesch, 1955), thus the high number of acidic cysteine residues in frusulins make them excellent substrates for metal binding. In our study, the limitation of N and/or P were responsible for the down-regulation of Fru5-1 gene expression and thus decreased the number of metal-binding sites, explaining why the nutrient-deficiency cells attracted fewer Cu^{2+} ions on their surfaces and the decrease of single-bonded form C-O in XPS analysis.

Effects of N and P on the Intracellular Response of *P. tricornutum* to Excess Cu

Enhanced metal sensitivity was not simply due to the accumulation of metal ions in the cells, especially in the organelles, but also resulted from the accumulation of cellular damage during the metal exposure period (Wang and Wang, 2011). In our study, Cu induced an increase in total protein and MDA content while causing a decrease in SOD activity in the N- and/or P-deficient cells relative to the control. It is thought that decreases in total soluble protein content under heavy metal stress may be due to an increase in protease activity (Palma et al., 2002), and that an increase in total soluble protein content under heavy metal stress may be related to the induced biosynthesis of stress proteins such as GSH and PCs (Verma and Dubey, 2003). Protein content significantly increases with increases in metal

concentration (Rastgoo and Alemzadeh, 2011). The decreased SOD activity in the cells with N and/or P shortages may indicate that the microalgae's antioxidative enzymatic system has been inhibited or destroyed due to more severe stress (Papadimitriou and Loumbourdis, 2002; Xia et al., 2015). Li et al. (2006) stated that the enhanced MDA content indicates that prolonged Cu exposure causes cell membrane damage under N- and/or P-limited conditions. Glutathione is the precursor for PCs, which are the first line of defense to combat against Cu-induced reactive oxygen species formation (Morelli and Scarano, 2004). A large number of experimental results have shown that after plants or cells are treated with heavy metals, the increase in PC content was associated with a corresponding decrease in GSH levels (Grill et al., 1985; Smith et al., 2014). Similarly, our study revealed that both the cells under N- and/or P-shortage conditions and those with sufficient N and P had a lower concentration of GSH after the Cu treatments, indicating that more PCs were synthesized to alleviate Cu stress in the diatoms, as previously found by Rijstenbil and Gerringa (2002). This result indicates that GSH can be used as a promising indicator of heavy-metal stress in plants and cells. However, the GSH content was not significantly different among the four treatments after Cu exposure. Therefore, more heavy metal chelators such as PCs and glutathione disulfide should be examined together, which could accurately reflect the oxidative stress status of the cells or the subcellular organelles.

CONCLUSION

In this study, we investigated the cellular defense mechanisms of the marine diatom *P. tricornutum* to cope with copper toxicity under different macronutrient (N and P) conditions. We found that cells under sufficient N and P conditions had more binding ligand on the cell walls and thus a larger proportion of metal was adsorbed to reduce metal toxicity. Correspondingly, when a N and/or P shortage was present, a weaker metal-ion exchange mechanism occurred to make up for the fewer number of cell surface metal ligands. The relatively higher levels of intracellular Cu in *P. tricornutum* cells under a N and/or P shortage induced

augmented protein synthesis and damaged the antioxidant enzyme system and membranes, which resulted in increased metal sensitivity.

DATA AVAILABILITY STATEMENT

The original contributions presented in the study are included in the article/**Supplementary Material**. Further inquiries can be directed to the corresponding author.

AUTHOR CONTRIBUTIONS

BZ: conceived and designed the research, performed the experiments, analyzed data, and wrote the manuscript. YZ, JM, and YL: performed the experiments and analyzed data. KP: conceived and designed the research and wrote the manuscript. All authors contributed to the article and approved the submitted version.

FUNDING

SUPPLEMENTARY MATERIAL

The Supplementary Material for this article can be found online at: https://www.frontiersin.org/articles/10.3389/fmars.2022.907114/full#supplementary-material

REFERENCES

Adams, M. S., Dillon, C. T., Vogt, S., Lai, B., Stauber, J., and Jolley, D. F. (2016). Copper Uptake, Intracellular Localization, and Speciation in Marine Microalgae Measured by Synchrotron Radiation X-Ray Fluorescence and Absorption Microspectroscopy. *Environ. Sci. Technol.* 50 (16), 8827–8839. doi: 10.1021/acs.est.6b00861

Alipanah, L., Winge, P., Rohloff, J., Najafi, J., Brembu, T., and Bones, A. M. (2018). Molecular Adaptations to Phosphorus Deprivation and Comparison With Nitrogen Deprivation Responses in the Diatom Phaeodactylum Tricornutum. *PLoS One* 13 (2), e0193335. doi: 10.1371/journal.pone.0193335

Armbrust, E. V., Berges, J. A., Bowler, C., Green, B. R., Martinez, D., Putnam, N. H., et al. (2004). The Genome of the Diatom Thalassiosira Pseudonana: Ecology, Evolution, and Metabolism. *Science* 06 (5693), 79–86. doi: 10.1126/science.1101156

Avery, S. V., and Tobin, J. M. (1993). Mechanism of Adsorption of Hard and Soft Metal Ions to Saccharomyces Cerevisiae and Influence of Hard and Soft Anions. *Appl. Environ. Microbiol.* 59 (9), 2851–2856. doi: 10.1128/aem.59.9.2851-2856.1993

Badruddoza, A., Tay, A., Tan, P., Hidajat, K., and Uddin, M. (2011). Carboxymethyl-β-Cyclodextrin Conjugated Magnetic Nanoparticles as Nano-Adsorbents for Removal of Copper Ions: Synthesis and Adsorption Studies. *J. Hazardous Materials* 185 (2-3), 1177–1186. doi: 10.1016/j.jhazmat.2010.10.029

Benesch, R. E., and Benesch, R. (1955). The Acid Strength of the -SH Group in Cysteine and Related Compounds. *J. Am. Chem. Soc.* 77 (22), 5877–5881. doi: 10.1021/ja01627a030

Blaby-Haas, C. E., and Merchant, S. S. (2012). The Ins and Outs of Algal Metal Transport. *Biochim. Biophys. Acta (BBA) - Mol. Cell Res.* 1823 (9), 1531–1552. doi: 10.1016/j.bbamcr.2012.04.010

Boukherroub, R., Morin, S., Sharpe, P., Wayner, D. D. M., and Allongue, P. (2000). Insights Into the Formation Mechanisms of Si-OR Monolayers From the Thermal Reactions of Alcohols and Aldehydes With Si(111)-H. *Langmuir* 16 (19), 7429e7434. doi: 10.1038/nature07410

Bowler, C., Allen, A. E., Badger, J. H., Grimwood, J., Jabbari, K., Kuo, A., et al. (2008). The Phaeodactylum Genome Reveals the Evolutionary History of Diatom Genomes. *Nature* 456 (7219), 239–244. doi: 10.1038/nature07410

Bradford, M. M. (1976). A Rapid and Sensitive Method for the Quantitation of Microgram Quantities of Protein Utilizing the Principle of Protein-Dye Binding. *Anal Biochem.* 72 (1), 248–254. doi: 10.1016/0003-2697(76)90527-3

Bræk, G. S., Malnes, D., and Jensen, A. (1980). Heavy Metal Tolerance of Marine Phytoplankton. IV. Combined Effect of Zinc and Cadmium on Growth and Uptake in Some Marine Diatoms. *J. Exp. Marine Biol. Ecol.* 42 (1), 39–54. doi: 10.1016/0022-0981(80)90165-3

Brembu, T., Chauton, M. S., Winge, P., Bones, A. M., and Vadstein, O. (2017). Dynamic Responses to Silicon in Thalasiossira Pseudonana - Identification, Characterisation and Classification of Signature Genes and Their Corresponding Protein Motifs. *Sci. Rep.* 7 (1), 1–14. doi: 10.1038/s41598-017-04921-0

Brembu, T., Jørstad, M., Winge, P., Valle, K. C., and Bones, A. M. (2011). Genome-Wide Profiling of Responses to Cadmium in the Diatom Phaeodactylum Tricornutum. *Environ. Sci. Technol.* 45 (18), 7640–7647. doi: 10.1021/es2002259

Bromke, M. A., Sabir, J. S., Alfassi, F. A., Hajarah, N. H., Kabli, S. A., Al-Malki, A. L., et al. (2015). Metabolomic Profiling of 13 Diatom Cultures and Their Adaptation to Nitrate-Limited Growth Conditions. *PLoS One* 10 (10), e0138965. doi: 10.1371/journal.pone.0138965

Campbell, P. M., and Smith, G. D. (1986). Transport and Accumulation of Nickel Ions in the Cyanobacterium Anabaena Cylindrica. *Arch.biochem.biophys* 244 (2), 470–477. doi: 10.1016/0003-9861(86)90615-6

Cicco, S. R., Vona, D., Gristina, R., Sardella, E., Ragni, R., Lo Presti, M., et al. (2016). Biosilica From Living Diatoms: Investigations on Biocompatibility of Bare and Chemically Modified Thalassiosira Weissflogii Silica Shells. *Bioengineering* 3 (4), 35. doi: 10.3390/bioengineering3040035

Compton, O., Jain, B., Dikin, D., Abouimrane, A., Amine, K., and Nguyen, S. (2011). Chemically Active Reduced Graphene Oxide With Tunable C/O Ratios. *ACS nano* 5, 4380–4391. doi: 10.1021/nn1030725

Condorelli, G. G., Motta, A., Fragala, I. L., Giannazzo, F., Raineri, V., Caneschi, A., et al. (2004). CAnchoring molecular magnets on the Si(100) surface. *Angew. Chem. Int. Ed* 43(31), 4081e4084. doi: 10.1002/anie.200453933

Conley, D. J., Paerl, H. W., Howarth, R. W., Boesch, D. F., Seitzinger, S. P., Havens, K. E., et al. (2009). Controlling Eutrophication: Nitrogen and Phosphorus. *Science* 323(5917), 1014. doi: 10.1126/science.1167755

De Riso, V., Raniello, R., Maumus, F., Rogato, A., Bowler, C., and Falciatore, A. (2009). Gene Silencing in the Marine Diatom Phaeodactylum Tricornutum. *Nucleic Acids Res.* 37 (14), e96–e96. doi: 10.1093/nar/gkp448

Dufrene, Y. F., Vander Wal, A., Norde, W., and Rouxhet, P. G. (1997). X-ray Photoelectron Spectroscopy Analysis of Whole Cells and Isolated Cell Walls of Gram-Positive Bacteria: Comparison With Biochemical Analysis. *J. Bacteriol* 179(4), 1023e1028. doi: 10.1128/jb.179.4.1023-1028.1997

Falkowski, P. G., Katz, M. E., Milligan, A. J., Fennel, K., Cramer, B. S., Aubry, M. P., et al. (2005). The Rise of Oxygen Over the Past 205 Million Years and the Evolution of Large Placental Mammals. *Science* 309(5744), 2202–2204. doi: 10.1126/science.1116047

Gélabert, A., Pokrovsky, O., Schott, J., Boudou, A., Feurtet-Mazel, A., and Mielczarski, J. (2004). Study of Diatoms/Aqueous Solution Interface. I. Acid-Base Equilibria and Spectroscopic Observation of Freshwater and Marine Species. *Geochim. Cosmochim. Ac.* 68 (15), 4039–58. doi: 10.1016/j.gca.2004.01.011

Gélabert, A., Pokrovsky, O., Schott, J., Boudou, A., and Feurtet-Mazel, A. (2007). Cadmium and Lead Interaction With Diatom Surfaces: A Combined Thermodynamic and Kinetic Approach. *Geochim Cosmochim Acta* 71 (15), 3698–3716. doi: 10.1016/j.gca.2007.04.034

Gélabert, A., Pokrovsky, O. S., Viers, J., Schott, J., Boudou, A., and Feurtet-Mazel, A. (2006). Interaction Between Zinc and Freshwater and Marine Diatom Species: Surface Complexation and Zn Isotope Fractionation. *Geochim Cosmochim Acta* 70 (4), 839–857. doi: 10.1016/j.gca.2005.10.026

Giannopolitis, C. N., and Ries, S. K. (1977). Superoxide Dismutases: I. Occurrence in Higher Plants. *Plant Physiol.* 59 (2), 309–314. doi: 10.1104/pp.59.2.309

Grill, E., Winnacker, E.-L., and Zenk, M. H. (1985). Phytochelatins: The Principal Heavy-Metal Complexing Peptides of Higher Plants. *Science* 230 (4726), 674–676. doi: 10.1126/science.230.4726.674

Hanikenne, M., Demoulin, V., and Baurain, D. (2005). A Comparative Inventory of Metal Transporters in the Green Alga Chlamydomonas Reinhardtii and the Red Alga Cyanidioschizon Merolae. *Plant Physiol.* 137 (2), 428–446. doi: 10.1104/pp.104.054189

Harrison, P., Thompson, P., and Calderwood, G. (1990). Effects of Nutrient and Light Limitation on the Biochemical Composition of Phytoplankton. *J. Appl. Phycol* 2 (1), 45–56. doi: 10.1007/BF02179768

Hasanuzzaman, M., Nahar, K., Anee, T. I., and Fujita, M. (2017). Glutathione in Plants: Biosynthesis and Physiological Role in Environmental Stress Tolerance. *Physiol. Mol. Biol. Plants* 23 (2), 249–268. doi: 10.1007/s12298-017-0422-2

He, J.-Y., Zhu, C., Ren, Y.-F., Yan, Y.-P., Cheng, C., Jiang, D.-A., et al. (2008). Uptake, Subcellular Distribution, and Chemical Forms of Cadmium in Wild-Type and Mutant Rice. *Pedosphere* 18 (003), 371–377. doi: 10.1016/S1002-0160(08)60027-2

He, C., Wang, L., Liu, J., Liu, X., Li, X., Ma, J, et al. (2013). Evidence for 'silicon' within the cell walls of suspension-cultured rice cells. *New Phytol* 200 (3), 700e709. doi: 10.1111/nph.12401

Jedlicka, S. S., Rickus, J. L., and Zemyanov, D. Y. (2007). Surface Analysis by X-ray Photoelectron Spectroscopy of Sol-gel Silica Modified With Covalently Bound Peptides. *J. Phys. Chem. B* 111 (40), 11850e11857. doi: 10.1021/jp0744230

Kim, S. A., Punshon, T., Lanzirotti, A., Li, L., Alonso, J. M., Ecker, J. R., et al. (2006). Localization of Iron in Arabidopsis Seed Requires the Vacuolar Membrane Transporter VIT1. *Science* 314 (5803), 1295. doi: 10.1126/science.1132563

Kröger, N., Bergsdorf, C., and Sumper, M. (1994). A New Calcium Binding Glycoprotein Family Constitutes a Major Diatom Cell Wall Component. *EMBO J.* 13 (19), 4676–4683. doi: 10.1002/j.1460-2075.1994.tb06791.x

Kröger, N., Bergsdorf, C., and Sumper, M. (1996). Frustulins: Domain Conservation in a Protein Family Associated With Diatom Cell Walls. *Eur. J. Biochem.* 239 (2), 259–264. doi: 10.1111/j.1432-1033.1996.0259u.x

Kröger, N., Lehmann, G., Rachel, R., and Sumper, M. (1997). Characterization of a 200-kDa Diatom Protein That Is Specifically Associated With a Silica-Based Substructure of the Cell Wall. *Eur. J. Biochem.* 250 (1), 99–105. doi: 10.1111/j.1432-1033.1997.00099.x

La Fontaine, S., and Mercer, J. F. B. (2007). Trafficking of the Copper-ATPases, ATP7A and ATP7B: Role in Copper Homeostasis. *Arch. Biochem. Biophys* 463 (2), 149–167. doi: 10.1016/j.abb.2007.04.021

Levy, J. L., Stauber, J. L., and Jolley, D. F. (2007). Sensitivity of Marine Microalgae to Copper: The Effect of Biotic Factors on Copper Adsorption and Toxicity. *Sci. Total Environ.* 387 (1-3), 141–154. doi: 10.1016/j.scitotenv.2007.07.016

Li, M., Hu, C., Zhu, Q., Chen, L., Kong, Z., and Liu, Z. (2006). Copper and Zinc Induction of Lipid Peroxidation and Effects on Antioxidant Enzyme Activities in the Microalga Pavlova Viridis (Prymnesiophyceae). *Chemosphere* 62 (4), 565–572. doi: 10.1016/j.chemosphere.2005.06.029

Lim, S.-F., Zheng, Y.-M., Zou, S.-W., and Chen, J. P. (2008). Characterization of Copper Adsorption Onto an Alginate Encapsulated Magnetic Sorbent by a Combined FT-IR, XPS, and Mathematical Modeling Study. *Environ. Sci. Technol.* 42 (7), 2551–2556. doi: 10.1021/es7021889

Litchman, E., Klausmeier, C., Miller, J., Schofield, O., and Falkowski, P. (2006). Multi-Nutrient, Multi-Group Model of Present and Future Oceanic Phytoplankton Communities. *Biogeosciences* 3 (4), 585–606. doi: 10.5194/bg-3-585-2006

Liu, S., Guo, Z., Li, T., Huang, H., and Lin, S. (2011). Photosynthetic Efficiency, Cell Volume, and Elemental Stoichiometric Ratios in Thalassirosira Weissflogii Under Phosphorus Limitation. *Chin. J. Oceanol Limnol* 29 (5), 1048–1056. doi: 10.1007/s00343-011-0224-2

Livak, K. J., and Schmittgen, T. D. (2001). Analysis of Relative Gene Expression Data Using Real-Time Quantitative PCR and the $2^{-\Delta\Delta CT}$ Method. *Methods* 25 (4), 402–408. doi: 10.1006/meth.2001.1262

Li, L. Z., Yu, S. Y., Peijnenburg, W. J. G. M., and Luo, Y. M. (2017). Determining the Fluxes of Ions (Pb^{2+}, Cu^{2+} and Cd^{2+}) at the Root Surface of Wetland Plants Using the Scanning Ion-Selective Electrode Technique. *Plant Soil* 414 (1), 1–12. doi: 10.1007/s11104-016-3109-5

Lu, H., Li, Z., Wu, J., Shen, Y., Li, Y., Zou, B., et al. (2017). Influences of Calcium Silicate on Chemical Forms and Subcellular Distribution of Cadmium in Amaranthus Hypochondriacus L. *Sci. Rep.* 7 (1), 1–9. doi: 10.1038/srep40583

Maldonado, M. T., and Price, N. M. (1996). Influence of N Substrate on Fe Requirements of Marine Centric Diatoms. *Marine Ecol. Prog. Ser.* 141, 161–172. doi: 10.3354/meps141161

Marella, T. K., Saxena, A., and Tiwari, A. (2020). Diatom Mediated Heavy Metal Remediation: A Review. *Bioresour Technol.* 305, 123068. doi: 10.1016/j.biortech.2020.123068

Ma, J., Zhou, B. B., Duan, D. D., Wei, Y., and Pan, K. (2018). Silicon Limitation Reduced the Adsorption of Cadmium in Marine Diatoms. *Aquat. Toxicol.* 202, 136–144. doi: 10.1016/j.aquatox.2018.07.011

Miao, A. J., and Wang, W. X. (2006). Cadmium Toxicity to Two Marine Phytoplankton Under Different Nutrient Conditions. *Aquat. Toxicol.* 78 (2), 114–126. doi: 10.1016/j.aquatox.2006.02.008

Miao, A.-J., and Wang, W.-X. (2007). Predicting Copper Toxicity With its Intracellular or Subcellular Concentration and the Thiol Synthesis in a Marine Diatom. *Environ. Sci. Technol.* 41 (5), 1777–1782. doi: 10.1021/es0613963

Milner, M. J., Seamon, J., Craft, E., and Kochian, L. V. (2013). Transport Properties of Members of the ZIP Family in Plants and Their Role in Zn and Mn Homeostasis. *J. Exp. Bot.* 64 (1), 369–381. doi: 10.1093/jxb/ers315

Misra, N., and Gupta, A. K. (2006). Effect of Salinity and Different Nitrogen Sources on the Activity of Antioxidant Enzymes and Indole Alkaloid Content in Catharanthus Roseus Seedlings. *J. Plant Physiol.* 163 (1), 11–18. doi: 10.1016/j.jplph.2005.02.011

Morelli, E., and Pratesi, E. (1997). Production of Phytochelatins in the Marine Diatom Phaeodactylum Tricornutum in Response to Copper and Cadmium Exposure. *Bull. Environ. contam Toxicol.* 59 (4), 657–664. doi: 10.1007/s001289900530

Morelli, E., and Scarano, G. (2004). Copper-Induced Changes of non-Protein Thiols and Antioxidant Enzymes in the Marine Microalga Phaeodactylum Tricornutum. *Plant Sci.* 167 (2), 289–296. doi: 10.1016/j.plantsci.2004.04.001

Nelson, D. M., Tréguer, P., Brzezinski, M. A., Leynaert, A., and Quéguiner, B. (1995). Production and Dissolution of Biogenic Silica in the Ocean: Revised Global Estimates, Comparison With Regional Data and Relationship to Biogenic Sedimentation. *Global Biogeochem Cycles* 9 (3), 359–372. doi: 10.1029/95GB01070

Nohira, H., Tsai, W., Besling, W., Young, E., Petry, J., Conard, T, et al (2002). Characterization of ALCVDAl2O3 and ZrO2 Layer Using X-ray Photoelectron Spectroscopy. *J. Non-Cryst. Solids* 303 (1), 83e87. doi: 10.1016/S0022-3093(02)00970-5

Palma, J. M., Sandalio, L. M., Corpas, F. J., Romero-Puertas, M. C., McCarthy, I., and Luis, A. (2002). Plant Proteases, Protein Degradation, and Oxidative Stress: Role of Peroxisomes. *Plant Physiol. Biochem.* 40 (6-8), 521–530. doi: 10.1016/S0981-9428(02)01404-3

Papadimitriou, E., and Loumbourdis, N. (2002). Exposure of the Frog Rana Ridibunda to Copper: Impact on Two Biomarkers, Lipid Peroxidation, and Glutathione. *Bull. Environ. contam Toxicol.* 69 (6), 0885–0891. doi: 10.1007/s00128-002-0142-2

Pistocchi, R., Mormile, M., Guerrini, F., Isani, G., and Boni, L. (2000). Increased Production of Extra-and Intracellular Metal-Ligands in Phytoplankton Exposed to Copper and Cadmium. *J. Appl. Phycol* 12 (3), 469–477. doi: 10.1023/A:1008162812651

Rastgoo, L., and Alemzadeh, A. (2011). Biochemical Responses of Gouan ('Aeluropus Littoralis') to Heavy Metals Stress. *Aust. J. Crop Sci.* 5 (4), 375–383. doi: 10.3316/informit.281334528451448

Raveendran, S., Chauhan, N., Palaninathan, V., Nagaoka, Y., Yoshida, Y., Maekawa, T, et al (2015). Extremophilic Polysaccharide for Biosynthesis and Passivation of Gold Nanoparticles and Photothermal Ablation of Cancer Cells. *Part. Part. Syst. Char.* 32 (1), 54e64. doi: 10.1002/ppsc.201400081

Rijstenbil, J., Dehairs, F., Ehrlich, R., and Wijnholds, J. (1998). Effect of the Nitrogen Status on Copper Accumulation and Pools of Metal-Binding Peptides in the Planktonic Diatom Thalassiosira Pseudonana. *Aquat. Toxicol.* 42 (3), 187–209. doi: 10.1016/S0166-445X(97)00091-X

Rijstenbil, J., and Gerringa, L. (2002). Interactions of Algal Ligands, Metal Complexation and Availability, and Cell Responses of the Diatom Ditylum Brightwellii With a Gradual Increase in Copper. *Aquat. Toxicol.* 56 (2), 115–131. doi: 10.1016/S0166-445X(01)00188-6

Rosenwasser, S., van Creveld, S. G., Schatz, D., Malitsky, S., Tzfadia, O., Aharoni, A., et al. (2014). Mapping the Diatom Redox-Sensitive Proteome Provides Insight Into Response to Nitrogen Stress in the Marine Environment. *Proc. Natl. Acad. Sci.* 111 (7), 2740–2745. doi: 10.1073/pnas.1319773111

Santos, J., Almeida, S. F. P., and Figueira, E. (2013). Cadmium Chelation by Frustulins: A Novel Metal Tolerance Mechanism in Nitzschia Palea (Kutzing) W. Smith. *Ecotoxicology* 22 (1), 166–173. doi: 10.1007/s10646-012-1013-1

Serra, A., Guasch, H., Admiraal, W., van der Geest, H., and Van Beusekom, S. (2010). Influence of Phosphorus on Copper Sensitivity of Fluvial Periphyton: The Role of Chemical, Physiological and Community-Related Factors. *Ecotoxicology* 19 (4), 770–780. doi: 10.1007/s10646-009-0454-7

Sivakumar, S., Song, Y., Park, I., Cho, S., Lee, C., and Kim, B. G. (2010). Short-Term Influence of Phosphate and Nitrate on Heavy Metal Accumulation by Red Alga Acrosorium Uncinatum. *Environ. monit Assess.* 165 (1), 449–460. doi: 10.1007/s10661-009-0958-x

Smith, C. L., Stauber, J. L., Wilson, M. R., and Jolley, D. F. (2014). The Use of Immobilised Metal Affinity Chromatography (IMAC) to Compare Expression of Copper-Binding Proteins in Control and Copper-Exposed Marine Microalgae. *Anal bioanal Chem.* 406 (1), 305–315. doi: 10.1007/s00216-013-7452-6

Takahashi, H., Kopriva, S., Giordano, M., Saito, K., and Hell, R. (2011). Sulfur Assimilation in Photosynthetic Organisms: Molecular Functions and Regulations of Transporters and Assimilatory Enzymes. *Annu. Rev. Plant Biol.* 62, 157–184. doi: 10.1146/annurev-arplant-042110-103921

Tesson, B., Genet, M. J., Fernandez, V., Degand, S., Rouxhet, P. G., Martin-Jézéqual, V, et al (2009). Surface chemical composition of diatoms. *Chembiochem* 10 (12), 2011–24. doi: 10.1002/cbic.200800811

Ting, Y., Lawson, F., and Prince, I. (1989). Uptake of Cadmium and Zinc by the Alga Chlorella Vulgaris: Part 1. *Individ. ion species.* 34 (7), 990–999. doi: 10.1002/bit.260340713

Verma, S., and Dubey, R. (2003). Lead Toxicity Induces Lipid Peroxidation and Alters the Activities of Antioxidant Enzymes in Growing Rice Plants. *Plant Sci.* 164 (4), 645–655. doi: 10.1016/S0168-9452(03)00022-0

Wang, W. X., and Dei, R. C. H. (2001). Metal Uptake in a Coastal Diatom Influenced by Major Nutrients (N, P, and Si). *Water Res.* 35 (1), 315–321. doi: 10.1016/S0043-1354(00)00256-6

Wang, W. X., and Dei, R. C (2006). Metal Stoichiometry in Predicting Cd and Cu Toxicity to a Freshwater Green Alga Chlamydomonas Reinhardtii. *Envir Poll.* 142 (2), 303–12. doi: 10.1016/j.envpol.2005.10.005

Wang, M. J., and Wang, W. X. (2008). Temperature-Dependent Sensitivity of a Marine Diatom to Cadmium Stress Explained by Subcelluar Distribution and Thiol Synthesis. *Environ. Sci. Technol.* 42 (22), 8603. doi: 10.1021/es801470w

Wang, M. J., and Wang, W. X. (2011). Cadmium Sensitivity, Uptake, Subcellular Distribution and Thiol Induction in a Marine Diatom: Exposure to Cadmium. *Aquat. Toxicol.* 101 (2), 377–386. doi: 10.1016/j.aquatox.2010.11.014

Weigel, H. J., and Jger, H. J. (1980). Subcellular Distribution and Chemical Form of Cadmium in Bean Plants. *Plant Physiol.* 65 (3), 480–482. doi: 10.1104/pp.65.3.480

Wu, Y., Yuan, Y., Yuan, H., Zhang, W., and Zhang, L. (2019). Predicting Cadmium Toxicity With the Kinetics of Phytochelatin Induction in a Marine Diatom. *Aquat. Toxicol.* 207, 101–109. doi: 10.1016/j.aquatox.2018.12.008

Xia, B., Chen, B., Sun, X., Qu, K., Ma, F., and Du, M. (2015). Interaction of TiO_2 Nanoparticles With the Marine Microalga Nitzschia Closterium: Growth Inhibition, Oxidative Stress and Internalization. *Sci. Total Environ.* 508, 525–533. doi: 10.1016/j.scitotenv.2014.11.066

Xin, L., Hong-Ying, H., Ke, G., and Ying-Xue, S. (2010). Effects of Different Nitrogen and Phosphorus Concentrations on the Growth, Nutrient Uptake, and Lipid Accumulation of a Freshwater Microalga Scenedesmus Sp. *Bioresour Technol.* 101 (14), 5494–5500. doi: 10.1016/j.biortech.2010.02.016

Yap, B. H., Crawford, S. A., Dagastine, R. R., Scales, P. J., and Martin, G. J. (2016). Nitrogen Deprivation of Microalgae: Effect on Cell Size, Cell Wall Thickness, Cell Strength, and Resistance to Mechanical Disruption. *J. Ind. Microbiol. Biotechnol.* 43 (12), 1671–1680. doi: 10.1007/s10295-016-1848-1

Zhao, Y., Tian, G., Duan, X., Liang, X., Meng, J., and Liang, J. (2019). Environmental Applications of Diatomite Minerals in Removing Heavy Metals From Water. *Ind. Eng. Chem. Res.* 58 (27), 11638–11652. doi: 10.1021/acs.iecr.9b01941

Zheng, J. C., Feng, H. M., Lam, M. H. W., Lam, P. K. S., Ding, Y. W., and Yu, H. Q. (2009). Removal of Cu (II) in Aqueous Media by Biosorption Using Water Hyacinth Roots as a Biosorbent Material. *J. Hazardous Materials* 171 (1-3), 780–785. doi: 10.1016/j.jhazmat.2009.06.078

Zhou, B., Ma, J., Chen, F., Zou, Y., Wei, Y., Zhong, H., et al. (2020). Mechanisms Underlying Silicon-Dependent Metal Tolerance in the Marine Diatom

Phaeodactylum Tricornutum. *Environ. Pollut* 262. doi: 10.1016/j.envpol.2020.114331

Conflict of Interest: The authors declare that the research was conducted in the absence of any commercial or financial relationships that could be construed as a potential conflict of interest.

Publisher's Note: All claims expressed in this article are solely those of the authors and do not necessarily represent those of their affiliated organizations, or those of the publisher, the editors and the reviewers. Any product that may be evaluated in

this article, or claim that may be made by its manufacturer, is not guaranteed or endorsed by the publisher.